

were reloaded. Among the pair of girders, one was provided with straight tendons while the other was provided with draped tendons. Such experimentation verified the existence of secondary moments from the application of prestress until attainment of peak load by the girder specimens. Besides, the experimental results reflected that the difference in prestress tendon eccentricities of the two girders led to differences in secondary moments and moment redistribution at central support sections.

Aravinthan et al. (2005) experimentally investigated the flexural behaviour of prestressed concrete continuous girders with highly eccentric external tendons, and the results revealed that the degree of moment redistribution at central support section is approximately proportional to the magnitude of secondary moment. Through theoretical derivations, Jian et al. (2001) postulated that if the plastic hinge at central support section of a prestressed concrete continuous beam has sufficient rotational capacity, full moment redistribution can occur and is unaffected by the secondary prestress moment. Conversely, if the plastic hinge does not have sufficient rotational capacity, the effect of secondary prestress moment on the moment redistribution should be considered. Normally, as the secondary moment is opposite to the external bending moment, this helps to increase the degree of moment redistribution.

2. DESIGN AND FABRICATION OF GIRDER SPECIMENS

The experimental investigation encompassed three externally prestressed concrete continuous girders with two equal spans. The girders were labelled specimen G-1, G-2 and G-3. The design parameters of the specimens were as follows: The effective prestress of external tendons was 900 MPa, the concrete grade was C40, the characteristic yield stress and tensile strength of main reinforcing bars were respectively 335 MPa and 455 MPa. The three girders had uniform cross section of 200 mm breadth and 300 mm height. The continuous girders had an overall length of 5200 mm, made up of two 2500 mm spans and 100 mm distance from each girder end to the side support. The specimens G-1, G-2 and G-3 were reinforced with grade HRB335 steel bars of 14 mm, 16 mm and 18 mm diameter, respectively. Grade HPB235 steel bars of 8 mm diameter were employed as shear stirrups. Fig. 1 illustrates the typical sections and reinforcement details of the girder specimens.

Each specimen was prestressed with two external tendons. The tendon had a nominal diameter of 15.24 mm and a nominal area of 140 mm² and was protected in plastic sheath. It had a yield stress of 1420 MPa and a tensile strength of 1860 MPa and the elastic modulus was 197 GPa. The profiles of external tendons were draped with three deviators locating at top side of the central support and bottom side of the two midspan sections. The tendon was anchored by wedge grips, and a pressure transducer was installed at the stressed end of each tendon. The specimens were loaded with concentrated vertical load exerted by hydraulic actuator at each midspan position. Fig. 2 depicts the load configuration and the external prestress tendon profile.

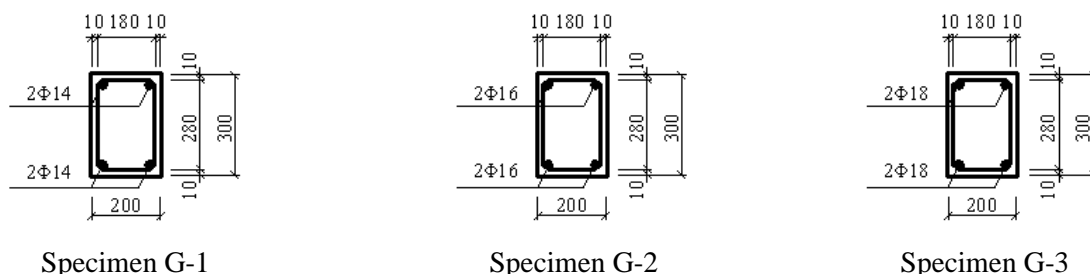


Fig. 1 Sections and reinforcement detail of specimens (dimensions in mm)

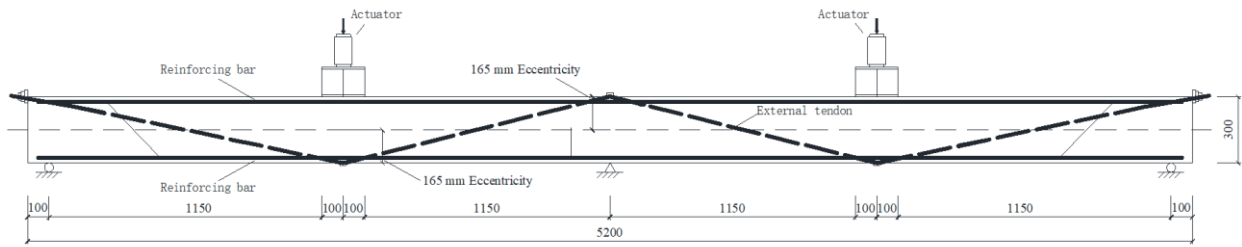


Fig. 2 External prestress tendon profile of specimens (dimensions in mm)

Table 1 Properties of reinforcing bars

Diameter (mm)	Sectional area (mm ²)	Yield stress (MPa)	Tensile strength (MPa)	Elastic modulus (GPa)
8	50.3	323.4	439.7	200
14	153.9	344.5	533.2	200
16	201.1	382.9	558.2	210
18	254.5	362.2	527.5	200

During preparation of reinforcing bars for the specimens, bar samples of 450 mm length were randomly cut from the reinforcement batches for carrying out tensile testing. The measured yield stresses from the bar samples are reported in Table 1. Along the main reinforcement embedded in the girder, the longitudinal strains were measured by strain gauges at central support section and midspan sections. At the instrumentation locations of strain gauges along the steel bar, the bar surface was locally ground and smoothed by abrasion wheel and sand-paper, and then cleaned and degreased by acetone wiped with cotton for adhering the strain gauges and sealing by paraffin, epoxy resin and fiberglass ribbon impregnated with epoxy resin.

The concrete was produced from ordinary Portland cement of strength grade 32.5, sand of particle size ranging from 0.35 to 0.5 mm as fine aggregate, and crushed gravel of particle size ranging from 5 to 20 mm as coarse aggregate. The mass ratio of cement : fine aggregate : coarse aggregate was 1 : 2.24 : 3.08, and the water to cement ratio was 0.58 by mass. For each girder specimen, 4 cube samples of 150 mm size were produced from the same batch of concrete and cured under the same conditions as the girder for compressive strength testing. The mean cube compressive strength of concrete for specimens G-1, G-2 and G-3 were measured as 55.3 MPa, 58.1 MPa and 52.8 MPa, respectively. After curing of concrete and at the date of testing, the girder was placed at the loading frame, and was instrumented with displacement gauges at support and mid-span locations, as well as strain gauges at concrete surface on the top of girder at two midspan sections.

The effective prestress of specimens G-1, G-2 and G-3 was 1071.2 MPa, 844.7 MPa and 878.8 MPa and the reinforcement index ρ_0 as calculated from Eq. (1) was 0.15, 0.14 and 0.17, respectively. In Eq. (1), f_{pe} is the effective prestress, A_p is nominal

area of tendon, f_y is the yield stress of reinforcing bar, A_s is the reinforcement area, f_c is the compressive strength of concrete, b is the breadth of girder and d_p is the distance between centroid of prestress tendon and extreme compression fibre of girder at critical section.

$$q_0 = \frac{f_{pe}A_p + f_yA_s}{f_c b d_p} \quad (1)$$

3. PROCEDURES OF LOAD TEST

The central support of continuous girder specimen was a fixed support, whereas the two side supports were roller supports. Each support was equipped with load cell and the height of support was adjustable. During initial positioning of girder specimen, the central support was lowered such that the girder was supported on the two side supports. The sum of load cell readings at side supports was equal to the self-weight of girder. Then, the central support was raised until the load cell readings at all supports corresponded to the theoretical support reactions of the continuous girder. Subsequently, displacement gauges and strain gauges were installed at appropriate locations of the girder specimen, and the instrumentations were connected to the data acquisition system.

Upon completion of the above setup, the external tendons were stressed gradually in three steps, a pause of 10 minutes was allowed between consecutive steps. After anchoring the tendons and a waiting time of 15 minutes, vertical loading was exerted from the hydraulic actuators to the midspan positions. Both actuators were controlled by a common hydraulic system and were synchronised. Fig. 3 depicts the load test of girder specimen. During the loading process, except the cracking of concrete was observed visually, the support reactions, tendon stresses, reinforcement strains, concrete strains and girder displacements were recorded automatically by the data acquisition system. The data were recorded at an interval of 2 to 5 kN increment of the total external load before appearance of signs of structural distress, thereafter the data were continually collected and recorded.

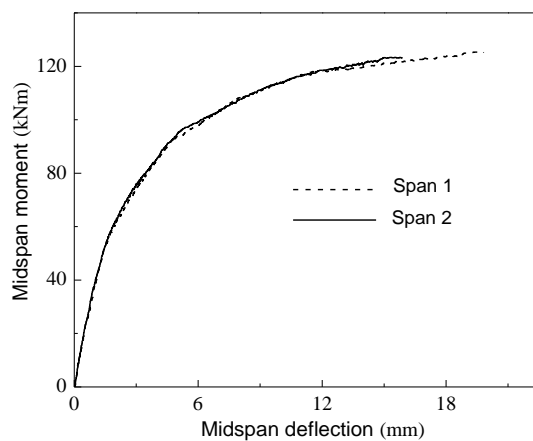


Fig. 3 Loading test of specimens

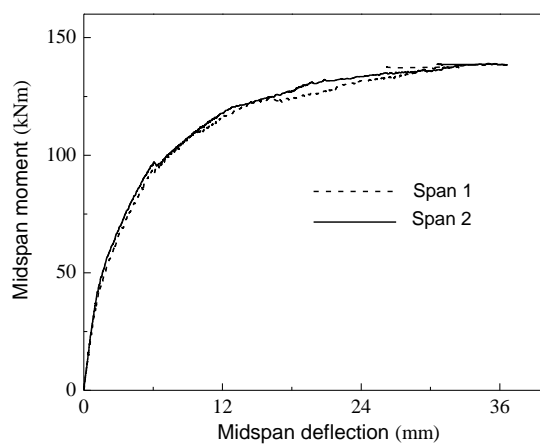
4. EXPERIMENTAL RESULTS

The moment-deflection curves of the girder specimens are plotted in Fig. 4, with the result for each span represented by an individual curve. Before concrete cracked, the girder was in elastic stage, the support reactions were in good match with the elastic analysis results. Upon cracking of concrete, the reaction at central support became smaller than the theoretical value, whereas the reactions at side supports became greater than the theoretical value. Upon yielding of main reinforcing bars under tension, the support reactions deviated further from the theoretical values until the girder attained the peak load. Fig. 5 plots the measured support reactions against the theoretical values for specimen G-3. The corresponding variations for specimens G-1 and G-2 were similar to those of G-3.

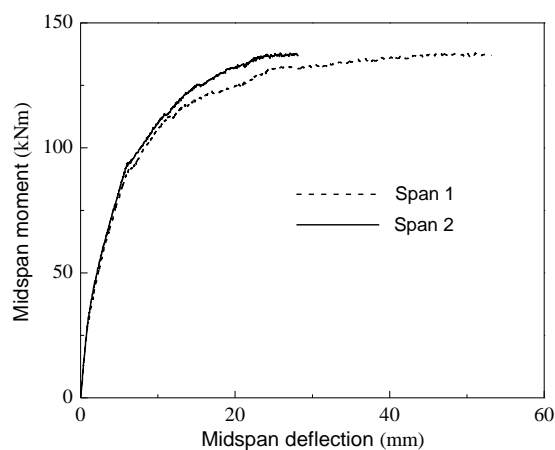
From the measured support reactions, the hogging moment at central support section and sagging moment at mid-span section of the girder specimen at various load levels can be computed. Fig. 6 plots the measured and theoretical bending moments at central support section and midspan sections against the applied load for specimen G-1. Fig. 7 and Fig. 8 plot the same relationships for specimens G-2 and G-3, respectively. These curves are inspected individually hereunder. From Fig. 6, it can be seen that when the applied load increased from 0 to 250 kN where the concrete began to crack, the measured bending moment was very close to the theoretical values. When the load increased to 450 kN where the main reinforcing bars yielded, the measured bending moment deviated from the theoretical values by -4.3 kNm (or -4%) and 1.8 kNm (or +2%) at central support section and mid-span section, respectively. Such deviations continued to increase when the girder specimen was further loaded, and reached respective difference of -22.9 kNm (or -12.8%) and 11.5 kNm (or +7.7%) at peak load of girder.



(a) Specimen G-1



(b) Specimen G-2



(c) Specimen G-3

Fig. 4 Moment-deflection curves of girder specimens

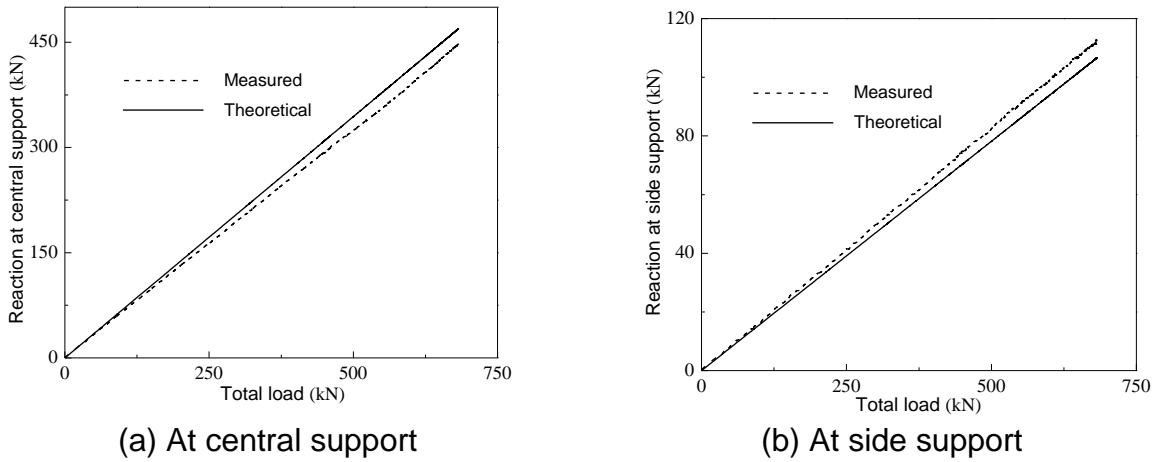


Fig. 5 Load-support reaction curves of specimen G-3

In Fig. 7 and Fig. 8, the curves corresponding to specimens G-2 and G-3 exhibit similar trends. For instance, from Fig. 8, it can be seen that when the applied load increased from 0 to 310 kN where the concrete began to crack, the measured bending moment was very close to the theoretical values. When the load increased to 470 kN where the reinforcing bars yielded, the measured bending moment deviated from the theoretical values by -11.7 kNm (or -6.6%) and 6.4 kNm (or +2.9%) at central support section and mid-span section, respectively. Such deviations continued to increase when the girder was further loaded, and reached respective difference of -30.7 kNm (or -14.6%) and 15.4 kNm (or +8.8%) at peak load of girder.

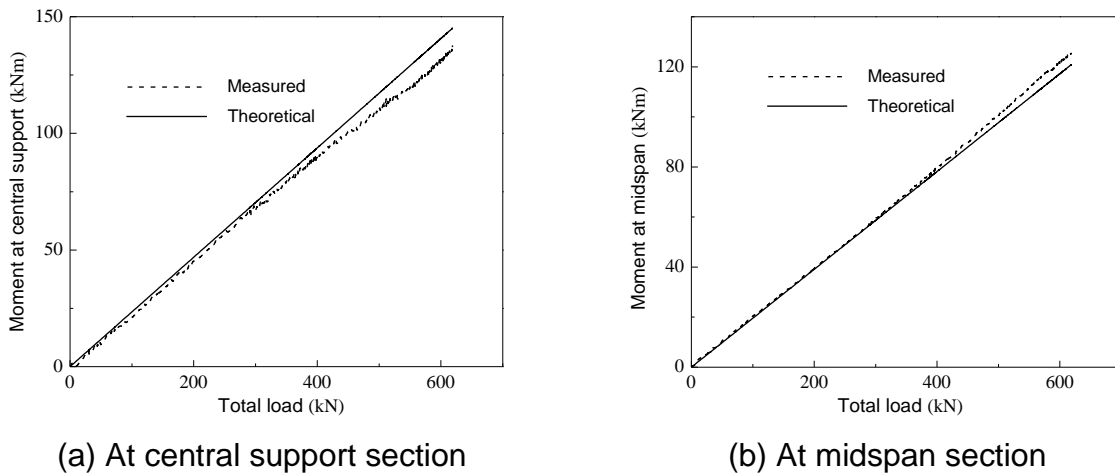
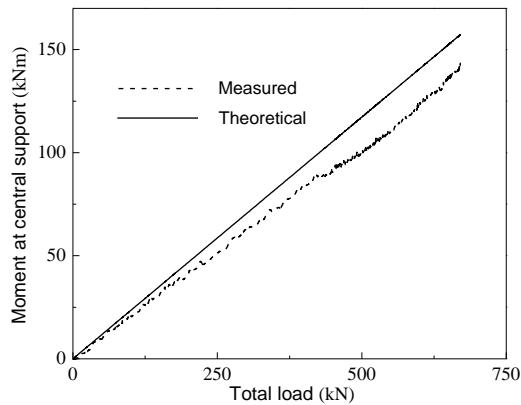
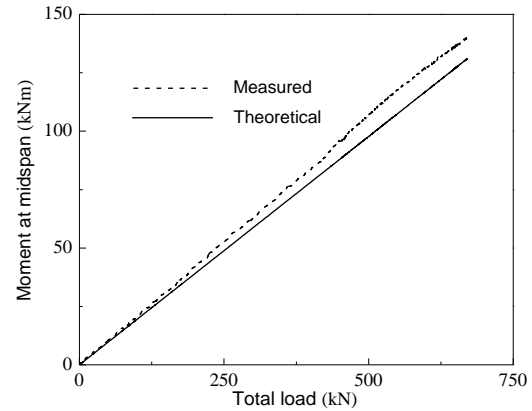


Fig. 6 Load-flexural moment curves of specimen G-1

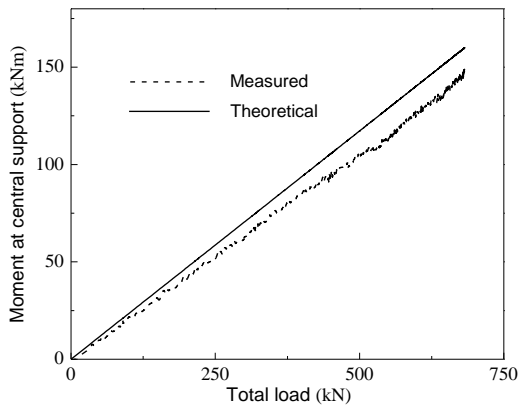


(a) At central support section

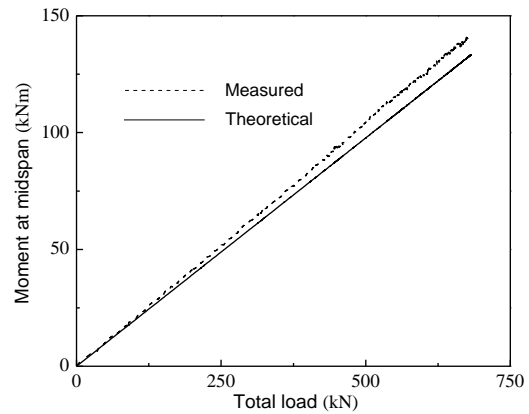


(b) At midspan section

Fig. 7 Load-flexural moment curves of specimen G-2



(a) At central support section



(b) At midspan section

Fig. 8 Load-flexural moment curves of specimen G-3

From the above, it is noted that the moment redistribution was the largest at peak load of the girder. Among specimens G-1, G-2 and G-3, the degree of moment redistribution was -12.8%, -16.9% and -14.6% at central support section, whereas the degree of moment redistribution was 7.7%, 10.2% and 8.8% at midspan section, respectively. Table 2 summarises the moment redistribution of the specimens. In the same table, the resulting prestress in tendons are listed. It can be seen that since the reinforcement index of the girder specimens was at the low side, the increase in ultimate stress of external tendons at peak load was relatively large and the ultimate stress exceeded the yield strength of 1420 MPa.

Table 2 Experimental results of girder specimens

Response	Section	Specimen		
		G-1	G-2	G-3
Secondary support reaction at stressing (kN)	Central support	-3.1	-2.5	-2.6
	Side support	+1.55	+1.25	+1.3
Average applied concentrated peak load (kN)	Midspan	383.0	423.6	448.4
Measured support reaction at peak load (kN)	Central support	508.2	555.6	592.0
	Side support	128.9	145.8	152.4
Theoretical flexural moment at peak load (kNm)	Central support	179.5	198.6	210.2
	Midspan	149.6	165.5	175.1
Actual flexural moment at peak load (kNm)	Central support	156.6	164.9	179.5
	Midspan	161.1	182.3	190.5
Percentage of moment redistribution (%)	Central support	-12.8	-16.9	-14.6
	Midspan	+7.7	+10.2	+8.8
Measured effective prestress (MPa)	External tendon	1071.2	844.7	878.8
Ultimate stress in tendons (MPa)	External tendon	1458.7	1622.4	1683.6

5. COMPARISON WITH DESIGN STANDARDS PROVISIONS

Comparative study is conducted between the moment redistribution behaviour manifested by the girder specimens and relevant provisions according to existing design standards. This enables to verify the applicability of codified design provisions to externally prestressed concrete continuous girders. In the following, denote α be the moment redistribution ratio at central support section, c be the depth of neutral axis, d be the distance between the centroid of main tension reinforcement and the extreme compression fibre of concrete, d_p be the distance between the centroid of prestress tendon and the extreme compression fibre of concrete, and β be the height of equivalent stress block of concrete under compression. The American Concrete Institute (ACI) suggested the below expression for evaluation of α in ACI 318-99 (ACI Committee 318, 1999):

$$\alpha \leq 20 \left(1 - 2.36 \frac{c}{d_p} \right) \quad (2)$$

The Canadian Standards Association (CSA) recommended α to be evaluated per Eq. (3), in accordance with A23.3-04 (CSA, 2004).

$$\alpha \leq 30 - 50 \frac{c}{d} \leq 20 \quad (3)$$

On the other hand, the British Standards Institution (BSI) put forward the following expression in British Standard BS 8110-2 (BSI, 1985):

$$\alpha \leq 50 - 100 \frac{c}{d} \leq 20 \quad (4)$$

According to the Chinese design standard GB 50010-2010 (MOHURD, 2010), assume the height of equivalent stress block of concrete is 0.8 times the depth of neutral axis, α can be evaluated as:

$$\alpha = 0.2 \left(1 - 2 \frac{c}{d} \right) \quad (5)$$

Based on the above four design standards, the moment redistribution ratios of girder specimens G-1, G-2 and G-3 are quantified and summarised in Table 3. It can be seen that the moment redistribution ratios calculated per ACI 318 for the 3 specimens are respectively 8.5%, 7.5% and 6.3%, all being less than the experimentally obtained values. The moment redistribution ratios calculated per A23.3-04 are respectively 17.1%, 15.9% and 14.4%, which match with the experimental results closely except specimen G-1. The moment redistribution ratios calculated per BS 8110-2 are respectively 20.0%, 20.0% and 18.8%, all being greater than the experimentally obtained values. Finally, the moment redistribution ratios calculated per GB 50010 are respectively 9.6%, 8.8% and 7.6%, all being smaller than the experimentally obtained values. Overall speaking, both ACI 318 and GB 50010 tend to be more conservative, A23.3-04 closely matches with the experimental results, while BS 8110-2 tends to be less conservative.

Table 3 Comparison of moment redistribution behaviour

Moment redistribution ratio	Specimen G-1	Specimen G-2	Specimen G-3
Experimental result	12.8%	16.9%	14.6%
ACI 318	8.5%	7.5%	6.3%
A23.3-04	17.1%	15.9%	14.4%
BS 8110-2	20.0%	20.0%	18.8%
GB 50010	9.6%	8.8%	7.6%
c/d_p ratio	0.24	0.26	0.29
c/d ratio	0.26	0.28	0.31

From the foregoing expressions and also from Table 3, it is observed that the moment redistribution ratio determined per design standards provisions decreases with increasing c/d_p or c/d . With the exception of specimen G-1, the experimentally obtained moment redistribution ratios of specimens G-2 and G-3 were lower at higher c/d_p or c/d ratio. It should be noted that in contrast to internally prestressed concrete girders with bonded tendons, the ultimate stress of unbonded tendons in externally prestressed concrete girders is related to the overall deformation of the member rather than individual sections. Normally, the ultimate stress of unbonded tendons would be less

than that of the bonded tendons, keeping other factors being equal. By substituting the ultimate prestress to evaluate the neutral axis depth, the case of unbonded tendons would give rise to a greater neutral axis depth. With reference to Eq. (2) to Eq. (5), compared to the case of bonded tendons, the larger value of c for unbonded tendons counterpart will lead to smaller value of α . This would be on the conservative side for hogging moments at internal support sections of continuous girder, but would be on the non-conservative side for sagging moments at midspan sections of continuous girder.

6. CONCLUSIONS

An experimental investigation has been conducted to examine the moment redistribution characteristics of three externally prestressed concrete continuous girder specimens with two equal spans subjected to concentrated loads at midspan positions. From the experimental results, before cracking of concrete, the support reactions and flexural response were close to elastic behaviour. After cracking of concrete, the measured central support reaction and the flexural moment thereat became less than those computed from elastic theory, whereas the measured side support reactions and the flexural moments at midspan sections became greater than those computed from elastic theory. Such deviations from the elastic theory further increased upon the yielding of reinforcing bars, and reached their maximum when the girder specimens attained the peak load. The experimentally obtained moment redistribution values of the 3 girder specimens were 12.8%, 16.9% and 14.6% respectively, and were all within 10% to 20%. The experimental results of moment redistribution were compared with the existing design standards provisions. It is found that American design standard ACI 318 and Chinese design standard GB 50010 tend to be more conservative, while British Standard BS 8110 tends to be less conservative. In contrast, Canadian Standard A23.3-04 matches closely with the experimental results. Lastly, in practical design of externally prestressed concrete continuous girders, reasonable ultimate stress in tendons should be adopted when codified equations are employed for the evaluation of moment redistribution.

ACKNOWLEDGEMENTS

The support by the European Commission under the Marie Skłodowska-Curie Actions (Project No. 751461) is gratefully acknowledged.

REFERENCES

ACI Committee 318 (1999), Building Code Requirements for Structural Concrete and Commentary (ACI 318M-99), American Concrete Institute, Farmington Hills, Michigan.

*The 2020 World Congress on
The 2020 Structures Congress (Structures20)
25-28, August, 2020, GECE, Seoul, Korea*

- Aravinthan, T., Witchukreangkrai, E. and Mutsuyoshi, H. (2005), "Flexural behavior of two-span continuous prestressed concrete girders with highly eccentric external tendons", *ACI Struct. J.*, **102**(3), 402-411.
- British Standards Institution (1985), *Structural Use of Concrete: Part 2, Code of Practice for Special Circumstances (BS 8110-2)*, British Standards Institution London.
- Canadian Standards Association (2004), *Design of Concrete Structures (A23.3-04)*, Canadian Standards Association, Mississauga, Ontario, Canada.
- Chan, E.K.H. and Au, F.T.K. (2015), "Behaviour of continuous prestressed concrete beams with external tendons", *Struct. Eng. Mech.*, **55**(6), 1099-1120.
- Du, J.S. and Liu, X.L (2008), "Experimental study of RC continuous beams strengthened by external prestressing", *Innovation and Sustainability of Modern Railway*, Proceedings of ISMR'2008, edited by X.Y. Lei, China Railway Publishing House, 221-227.
- Jian, B., Bai, S.L. and Wang, Z.L. (2001), "Ductility requirement in the moment redistribution of prestressed concrete continuous beams", *Eng. Mech.*, **18**(2), 51-57.
- Kodur, V.K.R. and Campbell, T.I. (1996), "Evaluation of moment redistribution in a two-span continuous prestressed concrete beam", *ACI Struct. J.*, **93**(6), 721-728.
- Lin, T.Y. and Thornton, K. (1972), "Secondary moment and moment redistribution in continuous prestressed concrete beams", *PCI J.*, **17**(1), 8-20.
- Lou, T.J., Lopes, S.M.R. and Lopes, A.V. (2014), "Factors affecting moment redistribution at ultimate in continuous beams prestressed with external CFRP tendons", *Compos. B Eng.*, **66**, 136-146.
- Lou, T.J., Liu, M.Y., Lopes, S.M.R. and Lopes, A.V. (2017), "Moment redistribution in two-span prestressed NSC and HSC beams", *Mater. Struct.*, **50**, 246.
- Lou, T.J., Peng, C.M., Karavasilis, T.L., Min, D. and Sun, W. (2020), "Moment redistribution versus neutral axis depth in continuous PSC beams with external CFRP tendons", *Eng. Struct.*, **209**, 109927.
- Mattock, A.H., Yamazaki, J. and Kattula, B.T. (1971), "Comparative study of prestressed concrete beams with and without bond", *ACI J.*, **68**(2), 116-125.
- Ministry of Housing and Urban-Rural Development of the People's Republic of China (MOHURD) (2010), *Code for Design of Concrete Structures (GB 50010-2010)*, China Architecture & Building Press, Beijing, China.
- Rebentrost, M. (2004), *Deformation Capacity and Moment Redistribution of Partially Prestressed Concrete Beams*, Ph.D. Thesis, Department of Civil and Environmental Engineering, University of Adelaide, Adelaide, Australia.
- Scott, R.H. and Whittle, R.T. (2005), "Moment redistribution effects in beams", *Mag. Concr. Res.*, **57**(1), 9-20.
- Scott, R.H., Whittle, R.T. and Azizi, A.R. (2007), "Measurement of moment redistribution effects in reinforced concrete beams", *Experimental Analysis of Nano and Engineering Materials and Structures*, edited by E.E. Gdoutos, Springer, Dordrecht, The Netherlands.
- Wyche, P.J., Uren, J.G. and Reynolds, G.C. (1993), "Interaction between prestress secondary moments, moment redistribution, and ductility—A treatise on the Australian concrete codes", *ACI Struct. J.*, **89**(1), 57-70.